Hindawi
Journal of Chemistry
Volume 2024, Article ID 6612503, 9 pages
https://doi.org/10.1155/2024/6612503

Research Article

Novel Xanthene-1,8-dione Derivatives Containing the Benzylic Ether Tail as Potent Cytotoxic Agents: Design, Synthesis, In Vitro, and In Silico Studies

Ahmad Ebadi,[1] Aref Karimi,[1] Asrin Bahmani,[1] Zahra Najafi,[2] and Gholamabbas Chehardoli [1]

[1]*Department of Medicinal Chemistry, School of Pharmacy, Medicinal Plants and Natural Products Research Center, Hamadan University of Medical Sciences, Hamadan, Iran*
[2]*Department of Medicinal Chemistry, School of Pharmacy, Hamadan University of Medical Sciences, Hamadan, Iran*

Correspondence should be addressed to Gholamabbas Chehardoli; cheh1002@gmail.com

Received 21 August 2023; Revised 25 December 2023; Accepted 27 December 2023; Published 5 January 2024

Academic Editor: James W. Gauld

Seventeen new xanthene-1,8-dione derivatives were synthesized and evaluated as cytotoxic agents against the lung carcinoma cell line (A549). Compound 9-(4-(benzyloxy)phenyl)-3,4,5,6,7,9-hexahydro-1H-xanthene-1,8(2H)-dione (**4a**) showed good cytotoxic effects (34.59 μM) in comparison to cis-platin. Docking results showed **4a** could interact with DNA as intercalation. Calculated ligand efficiency of compound **4a** was more than daunomycin. Based on the results, it can be concluded that compound **4a** is a suitable DNA binding agent.

1. Introduction

Today, cancer has become a big problem for the treatment systems of countries due to its widespread prevalence and the difficulty of treatment. Comprehensive studies have been conducted to determine the causes, prevention, and treatment of this disease [1]. DNA chain is known as the cellular target of many anticancer compounds. The interaction of a drug with the DNA chain has a special role in the pharmacological effects as well as the mechanism of action of that drug. Understanding how the complex affects both the mechanical and structural properties of DNA is an important step toward elucidating the functional mechanism of binding agents and may also provide information for more selective drug design [2].

Drug binding to the DNA chain can be classified into two general categories: covalent interactions and noncovalent interactions. The most important examples of covalent interactions are DNA-alkylating drugs. The main advantage of alkylating compounds is their high binding power to the nucleotide bases of the DNA chain. As a result of alkylation, the DNA chain undergoes structural changes that affect both transcription and replication processes [3]. Temozolomide (**I**), carmustine (**II**), and cyclophosphamide (**III**) are three famous examples of DNA alkylating drugs (Figure 1) [4].

Noncovalent interactions are divided into two categories. DNA grooves Interacting agents and intercalating agents. Some small chemical compounds are attached to the minor groove of DNA by forming van der Waals and hydrogen bonds. These molecules deform the DNA by binding to the minor groove and disrupting DNA function [5]. Berenil (**IV**) is an example of these compounds [6]. Due to the formation of π-π interactions with DNA nucleotide bases, intercalators are placed perpendicular to the DNA chain and between nucleotide bases. Intercalator drugs cause a change in the twist of DNA and cause a change in function, leading to the inhibition of transcription, replication, and repair processes in DNA [7]. Daunomycin (**V**) is an intercalating agent [8].

Xanthenes are a family of oxygen-containing heterocycles. The pyran ring is the central building block of them.

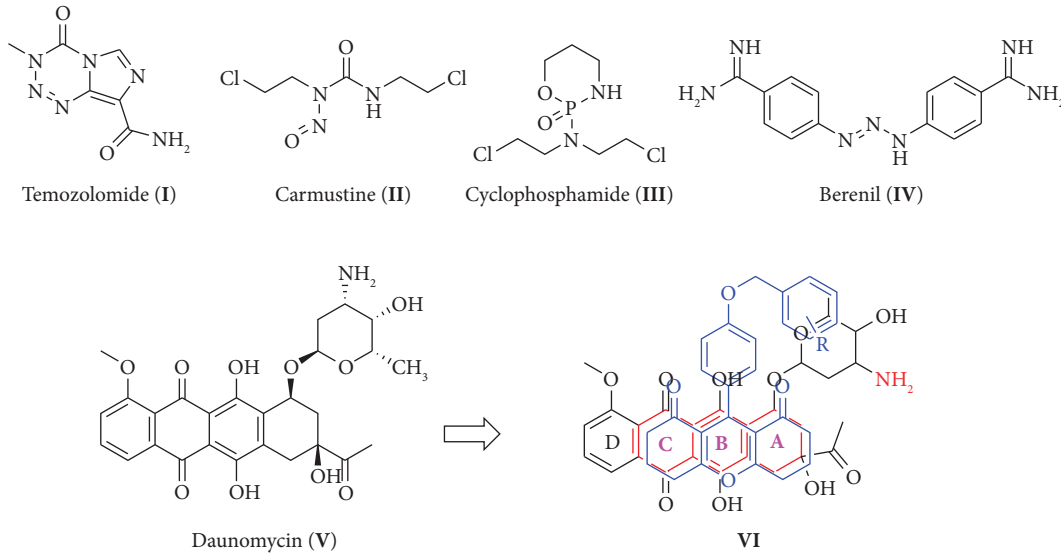

Figure 1: Structure of some covalent (I–III) and noncovalent (IV and V) DNA binding agents. Overlay of Daunomycin (red) and synthesized general xanthene-1,8-dione derivative (blue) showed that the tricyclic system matched with the A-B-C ring system in Daunomycin.

Xanthene derivatives have a broad range of biological activities, such as antioxidative, antihypertensive, antithrombotic, and anticancer activity [9–11]. Among the different types of xanthenes, xanthene-1,8-diones have shown promising activities in the field of anticancer research. Especially the xanthene-1,8-diones derivatives showed good antitumor effects against the human lung cancer cell line (A549) [12].

The tricyclic ring system of xanthene-1,8-diones resembles the A-B-C ring system in anthracyclines such as daunomycin (**VI** in Figure 1). As Figure 1 shows, if there is a suitable basic substitution in the benzyl or phenoxy moieties, it has the same orientation as the amino group in the aminoglycoside of Daunomycin. The similarity between the ring systems of these two classes of anticancer agents prompted us to investigate the interaction of xanthene-1,8-dione derivatives with DNA chain.

In continuation of our studies on biologically active heterocycles [13–16], especially the synthesis of DNA binding agents [17], a series of novel xanthene-1,8-diones derivatives were synthesized and evaluated for their cytotoxic activities.

2. Materials and Methods

2.1. Materials and Instrumental. Chemical substances were purchased from Merck and Sigma. Uncorrected melting points were measured by a Stuart SMP3 apparatus. An alpha-BRUKER IR device recorded the IR spectra of products on KBr disks. A Bruker 500-NMR spectrometer recorded the ^{1}H NMR spectra. An Agilent technology (HP 5975C MSD) mass spectrometer operating at an ionization potential of 70 eV, recorded the mass spectra of the products. The A549 cancer cell line was purchased from the Pasteur Institute of Iran (IPI). PBS, FBS, RPMI, trypsin-EDTA, and Pen-strep were prepared from Kiazist Company.

2.2. General Procedure for the Synthesis of Xanthene-1,8-dione Derivatives Containing the Benzylic Ether Tail. 4-(Benzyloxy)benzaldehyde derivatives were synthesized as per the previous reported method [17]. In a 25 mL round-bottom flask, 4-(benzyloxy)benzaldehyde derivatives **3** (1 mmol) and 2 mmol 1,3-cyclohexanedione were added to 3 mL ethylene glycol. Then the reaction mixture was stirred at 80°C for 24 hours. After the reaction was complete, a water/ice mixture was added to the reaction mixture to precipitate the products. The precipitate was washed with the boiling CH_3OH. For further purification, it was recrystallized with methanol.

2.3. Physical and Spectral Data of Products

4a: 9-(4-(Benzyloxy)phenyl)-3,4,5,6,7,9-hexahydro-1H-xanthene-1,8(2H)-dione

White solid

Yield: 75%

Melting point: 204–207°C

^{1}H NMR (500 MHz, DMSO-d_6) δ: 7.59–7.20 (m, 5H), 7.07 (d, J = 8.1 Hz, 2H), 6.89–6.74 (d, J = 8.1 Hz, 2H), 5.00 (s, 2H), 4.51 (s, 1H), 2.62 (m, 4H), 2.25 (m, 4H), 1.97–1.76 (m, 4H). IR (KBr, cm^{-1}) v: 2947.72, 1671.85, 1509.41, 1176.56, 1133.59; MS m/z (%): 91 (100), 217 (67.9), 309.2 (53.6), 400.3 (41).

4b: 9-(4-((4-Bromobenzyl)oxy)phenyl)-3,4,5,6,7,9-hexahydro-1H-xanthene-1,8(2H)-dione

White solid

Yield: 71%

Melting point: 218–223°C

^{1}H NMR (300 MHz, DMSO-d_6) δ: 7.66–7.49 (d, J = 9 Hz, 2H), 7.44–7.31 (d, J = 9 Hz, 2H), 7.15–6.99 (d, J = 6 Hz, 2H), 6.89–6.74 (d, J = 6 Hz, 2H),

5.00 (s, 2H), 4.52 (s, 1H), 2.72–2.55 (m, 4H), 2.41–2.17 (m, 4H), 2.03–1.74 (m, 4H). IR (KBr, cm^{-1}) ν: 2937.28, 1671.46, 1505.59, 1171.59, 1129.01; MS m/z (%): 90.3 (20), 69 (76.9), 217.3 (100), 309.2 (64.6), 478.3 (11.9), 480.3 (12.3).

4c: 9-(4-((3-Chlorobenzyl)oxy)phenyl)-3,4,5,6,7,9-hexahydro-1H-xanthene-1,8(2H)-dione

White solid

Yield: 65%

Melting point: 202–205°C

^{1}H NMR (300 MHz, DMSO-d_6) δ: 7.54–7.31 (d, J = 27 Hz, 4H), 7.10 (d, J = 8.4 Hz, 2H), 6.84 (d, J = 8.4 Hz, 2H), 5.03 (s, 2H), 4.53 (s, 1H), 2.61 (m, 4H), 2.27 (m, 4H), 1.89 (m, 4H). IR (KBr, cm^{-1}) ν: 2945.45, 1670.19, 1510.01, 1181.40, 1132.59; MS m/z (%): 125.2 (64.6), 217.3 (100), 309.2 (82.9), 434.3 (37.8), 436.13 (12.1).

4d: 9-(4-((4-Fluorobenzyl)oxy)phenyl)-3,4,5,6,7,9-hexahydro-1H-xanthene-1,8(2H)-dione

White solid

Yield: 63%

Melting point: 176–179°C

^{1}H NMR (300 MHz, DMSO-d_6) δ: 7.50–7.39 (m, 2H), 7.23–7.14 (t, J = 6 Hz, 2H), 7.12–7.02 (d, J = 9 Hz, 2H), 6.89–6.77 (d, J = 6 Hz, 2H), 4.98 (s, 2H), 4.51 (s, 1H), 2.71–2.51 (m, 4H), 2.33–2.15 (m, 4H), 2.01–1.71 (m, 4H). IR (KBr, cm^{-1}) ν: 2955,88, 1666.18, 1513.46, 1175.53, 1129.64; MS m/z (%): 109.3 (100), 217.3 (63.6), 309.2 (41.45), 418.4 (29).

4e: 9-(4-((2-Fluorobenzyl)oxy)phenyl)-3,4,5,6,7,9-hexahydro-1H-xanthene-1,8(2H)-dione

White solid

Yield: 58%

Melting point: 195–198°C

^{1}H NMR (300 MHz, DMSO-d_6) δ: 7.52 (t, J = 7.5, 1.7 Hz,1H), 7.45–7.35 (m, 1H), 7.28–7.18 (m, 2H), 7.14–7.06 (d, J = 6 Hz, 2H), 6.90–6.83 (d, J = 6 Hz, 2H), 5.05 (s, 2H), 4.54 (s, 1H), 2.74–2.53 (m, 4H), 2.37–2.18 (m, 4H), 1.89 (m, 4H). IR (KBr, cm^{-1}) ν: 2950.80, 1673.07, 1510.93, 1178.70, 1130.54; MS m/z (%): 109.3 (83.7), 217.3 (100), 309.2 (55.6), 418.4 (43.3).

4f: 9-(4-((3-Fluorobenzyl)oxy)phenyl)-3,4,5,6,7,9-hexahydro-1H-xanthene-1,8(2H)-dione

White solid

Yield: 48%

Melting point: 200–203°C

^{1}H NMR (300 MHz, DMSO-d_6) δ: 7.38 (m, 1H), 7.27–7.16 (m, 2H), 7.15–7.07 (m, 1H), 7.08–7.02 (d, J = 9 Hz, 2H), 6.86–6.73 (d, J = 9 Hz, 2H), 5.00 (s, 2H), 4.49 (s, 1H), 2.69–2.48 (m, 4H), 2.33–2.13 (m, 4H), 1.97–1.71 (m, 4H). IR (KBr, cm^{-1}) ν: 2947.92, 1671.13, 1510.16, 1180.10, 1131.24; MS m/z (%): 109.3 (66.3), 217.3 (100), 309.3 (96.3), 418.4 (61).

4g: 9-(4-((4-Methylbenzyl)oxy)phenyl)-3,4,5,6,7,9-hexahydro-1H-xanthene-1,8(2H)-dione

Red solid

Yield: 42%

Melting point: 218–222°C

^{1}H NMR (300 MHz, DMSO-d_6) δ: 7.29 (d, J = 7.9 Hz, 2H), 7.17 (d, J = 7.9 Hz, 2H), 7.10–7.03 (d, J = 9 Hz, 2H), 6.87–6.75 (d, J = 9 Hz, 2H), 4.96 (s, 2H), 4.51 (s, 1H), 2.72–2.54 (m, 4H), 2.34–2.21 (m, 7H), 2.02–1.74 (m, 4H). IR (KBr, cm^{-1}) ν: 2952.40, 1668.71, 1508.38, 1176.62, 1128,91; MS m/z (%): 105.3 (100), 217.2 (83.8), 309.3 (98), 418.4 (61), 414.4 (28.5).

4h: 9-(4-((4-Chlorobenzyl)oxy)phenyl)-3,4,5,6,7,9-hexahydro-1H-xanthene-1,8(2H)-dione

White solid

Yield: 70%

Melting point: 215–218°C

^{1}H NMR (300 MHz, DMSO-d_6) δ: 7.46 (s, 4H), 7.16–7.05 (d, J = 9 Hz, 2H), 6.91–6.80 (d, J = 9 Hz, 2H), 5.04 (s, 2H), 4.55 (s, 1H), 2.74–2.55 (m, 4H), 2.39–2.20 (m, 4H), 2.04–1.76 (m, 4H). IR (KBr, cm^{-1}) ν: 2967.09, 1671.41, 1505.74, 1172.10, 1128.82; MS m/z (%): 125.2 (100), 217.3 (72.76), 309.2 (55.9), 434.3 (23.68), 436.13 (7.9).

4i: 9-(4-(Benzyloxy)-3-methoxyphenyl)-3,4,5,6,7,9-hexahydro-1H-xanthene-1,8(2H)-dione

White solid

Yield: 64%

Melting point: 172–175°C

^{1}H NMR (300 MHz, DMSO-d_6) δ: 7.42–7.24 (m, 5H), 6.86–6.74 (m, 2H), 6.58 (d, J = 3 Hz, 1H), 4.95 (s, 2H), 4.51 (s, 1H), 3.68 (s, 3H), 2.69–2.47 (m, 4H), 2.36–2.15 (m, 4H), 2.01–1.70 (m, 4H). IR (KBr, cm^{-1}) ν: 2942.01, 1661.04, 1513.78, 1174.71, 1141.21; MS m/z (%): 64.2 (100), 91.2 (53.1), 217.2 (33.8), 304.3 (48.8), 430.4 (14.6).

4j: 9-(4-((4-Bromobenzyl)oxy)-3-methoxyphenyl)-3,4,5,6,7,9-hexahydro-1H-xanthene-1,8(2H)-dione

Yellow solid

Yield: 52%

Melting point: 185–189°C

^{1}H NMR (300 MHz, DMSO-d_6) δ: 7.66–7.56 (d, J = 9 Hz, 2H), 7.45–7.34 (d, J = 9 Hz, 2H), 6.90–6.79 (d, J = 6 Hz, 2H), 6.65 (dd, J = 3 Hz, 1H), 5.00 (s, 2H), 4.59 (s, 1H), 3.75 (s, 3H), 2.75–2.52 (m, 4H), 2.39–2.19 (m, 4H), 2.05–1.73 (m, 4H). IR (KBr, cm^{-1}) ν: 2937.97, 1589.21, 1509.65, 1191.91, 1138.15; MS m/z (%): 109.2 (44.6), 169.2 (55.1), 217.3 (100), 292.1 (50.6), 462.2 (17), 508.3 (2.9), 510.3 (3.4).

4k: 9-(4-((3-Chlorobenzyl)oxy)-3-methoxyphenyl)-3,4,5,6,7,9-hexahydro-1H-xanthene-1,8(2H)-dione

Red solid

Yield: 67%

Melting point: 144–147°C

^{1}H NMR (300 MHz, DMSO-d_6) δ: 7.53–7.33 (m, 4H), 6.91–6.81 (d, J = 9 Hz, 2H), 6.65 (dd, J = 3 Hz, 1H), 5.03 (s, 2H), 4.57 (s, 1H), 3.75 (s, 3H), 2.75–2.54 (m, 4H), 2.39–2.22 (m, 4H), 2.07–1.78 (m, 4H). IR (KBr, cm^{-1}) v: 2945.85, 1659.47, 1511.52, 1176.48, 1141.52; MS m/z (%): 64.2 (100), 125.2 (54.4), 217.3 (81.3), 339.3 (32.8), 464.4 (14.9), 466.4 (4.9).

4l: 9-(4-((4-Fluorobenzyl)oxy)-3-methoxyphenyl)-3,4,5,6,7,9-hexahydro-1H-xanthene-1,8(2H)-dione

White solid

Yield: 61%

Melting point: 145–150°C

^{1}H NMR (300 MHz, DMSO-d_6) δ: 7.51–7.35 (m, 2H), 7.24–7.09 (t, J = 9 Hz, 2H), 6.86–6.75 (m, 2H), 6.58 (dd, J = 3 Hz, 1H), 4.93 (s, 2H), 4.51 (s, 1H), 3.68 (s, 3H), 2.58 (m, 4H), 2.33–2.14 (m, 4H), 1.98–1.73 (m, 4H). IR (KBr, cm^{-1}) v: 2958.38, 1654.69, 1516.65, 1172.74, 1130.02; MS m/z (%): 109.2 (81.5), 217.2 (100), 279.3 (50), 339.3 (49), 448.4 (23).

4m: 9-(4-((2-Fluorobenzyl)oxy)-3-methoxyphenyl)-3,4,5,6,7,9-hexahydro-1H-xanthene-1,8(2H)-dione

Brown solid

Yield: 54%

Melting point: 155–158°C

^{1}H NMR (300 MHz, DMSO-d_6) δ: 7.54 (m, 1H), 7.43 (m, 1H), 7.32–7.19 (m, 2H), 6.97–6.81 (m, 2H), 6.67 (dd, J = 3 Hz, 1H), 5.05 (s, 2H), 4.58 (s, 1H), 3.73 (s, 3H), 2.78–2.52 (m, 4H), 2.43–2.22 (m, 4H), 2.07–1.77 (m, 4H). IR (KBr, cm^{-1}) v: 2945.90, 1655.01, 1513.20, 1173.37, 1130.93; MS m/z (%): 109.2 (100), 217.2 (82.8), 340.3 (47.8), 448.4 (13.9).

4n: 9-(4-((3-Fluorobenzyl)oxy)-3-methoxyphenyl)-3,4,5,6,7,9-hexahydro-1H-xanthene-1,8(2H)-dione

White solid

Yield: 63%

Melting point: 160–163°C

^{1}H NMR (300 MHz, DMSO-d_6) δ: 7.45 (m, 1H), 7.30–7.22 (m, 2H), 7.21–7.13 (m, 1H), 6.89–6.83 (m, 2H), 6.65 (dd, J = 3 Hz, 1H), 5.04 (s, 2H), 4.57 (s, 1H), 3.75 (s, 3H), 2.77–2.54 (m, 4H), 2.36–2.22 (m, 4H), 1.93 (m, 4H). IR (KBr, cm^{-1}) v: 2952.16, 1658.96, 1513.16, 1175.52, 1141.55; MS m/z (%): 64.2 (100), 109.2 (77), 217.2 (52.7), 279.3 (34.5), 339.3 (38.7), 448.4 (31).

4o: 9-(3-Methoxy-4-((4-methylbenzyl)oxy)phenyl)-3,4,5,6,7,9-hexahydro-1H-xanthene-1,8(2H)-dione

White solid

Yield: 28%

Melting point: 129–132°C

^{1}H NMR (300 MHz, DMSO-d_6) δ: 7.26 (d, J = 7.9 Hz, 2H), 7.14 (d, J = 7.9 Hz, 2H), 6.84–6.73 (m, 2H), 6.57 (dd, J = 3 Hz, 1H), 4.91 (s, 2H), 4.50 (s, 1H), 3.68 (s, 3H), 2.72–2.50 (m, 4H), 2.26 (m, 7H), 1.98–1.75 (m, 4H). IR (KBr, cm^{-1}) v: 2949.14, 1661.07, 1512.74, 1177.25,1142.98; MS m/z (%): 105.1 (100), 217.2 (26.1), 397.3 (13.8), 444.3 (3.8).

4p: 9-(4-((4-Chlorobenzyl)oxy)-3-methoxyphenyl)-3,4,5,6,7,9-hexahydro-1H-xanthene-1,8(2H)-dione

White solid

Yield: 70%

Melting point: 146–149°C

^{1}H NMR (300 MHz, DMSO-d_6) δ: 7.44 (s, 4H), 6.87–6.78 (m, 2H), 6.61 (dd, J = 3 Hz, 1H), 4.99 (s, 2H), 4.54 (s, 1H), 3.72 (s, 3H), 2.72–2.53 (m, 4H), 2.35–2.22 (m, 4H), 1.91 (m, 4H). IR (KBr, cm^{-1}) v: 2956.23, 1655.30, 1513.43, 1172.87, 1128.95; MS m/z (%): 64.2 (100), 125.2 (80), 217.2 (69.1), 248.2 (70.4), 372.3 (34.2), 464.3 (4), 466.3 (1.3).

4q: 4-((4-(1,8-Dioxo-2,3,4,5,6,7,8,9-octahydro-1*H*-xanthen-9-yl)phenoxy)methyl)benzonitrile

Red solid

Yield: 52%

Melting point: 193–198°C

^{1}H NMR (301 MHz, DMSO-d_6) δ: 7.96–7.84 (d, J = 8.2 Hz, 2H), 7.63 (d, J = 8.2 Hz, 2H), 7.19–7.08 (d, J = 9 Hz, 2H), 6.91–6.84 (d, J = 9 Hz, 2H), 5.15 (s, 2H), 4.55 (s, 1H), 2.63 (m, 4H), 2.38–2.13 (m, 4H), 2.03–1.75 (m, 4H). IR (KBr, cm^{-1}) v: 2941.85, 2225.10, 1670.79, 1506.43, 1173.28,129.03; MS m/z (%): 116.2 (61), 217.2 (66), 309.3 (100), 425.4 (46.1).

2.4. Biological Evaluation

2.4.1. In Vitro Cytotoxicity. The human was used for cell viability tests. Cells were grown in high glucose DMEM medium supplemented with 10% FBS (fetal bovine Serum) and 1% (V/V) penicillin-streptomycin in a 95% humidified medium with 5% CO_2. Cell survival was evaluated using the MTT assay. Concisely, the total number of 10^4 A549 cells was precultured in each well of a 96-well plate. After 16 hours incubation, various concentrations of the substance (12.5, 25, 50, and 100 μM) were incubated for 72 hours. After an appropriate time, a fresh medium with MTT solution at a final concentration of 0.50 mg/ml was added to each well and incubated for an extra 4 hours under the same condition. At the final point, the solvent buffer including a culture medium was removed, and 100 μL of 100% DMSO was used to dissolve the produced crystalline formazan. Then, the absorbances of the samples were read by the BMG Spectro-Nano Elizabeth Reader at two wavelengths of 570 and 630 nm, relating to the formazan and background absorbance. The percentage of live cells was determined using the formula: cell viability % = [AT (sample)/AT (control)] × 100, where the AT is defined as $A_{570}-A_{630}$. The viability percentage was estimated as the mean ± standard deviation (STDEV) from 3 independent experiments. The IC_{50} values were calculated by GraphPad Prism9.0 software.

2.5. In Silico Studies. The structure of Daunomycin in complex with DNA chain (PDB code: 1d11, resolution: 1.18 Å) was downloaded from the RCSB database [18]. The water molecules were removed, and the Daunomycin and apo form of DNA saved in pdb format separately. The molecular docking procedure and ADME prediction were performed according to our previously reported paper [17].

3. Results and Discussion

3.1. Chemistry. In a previous study, the synthesis and interactions of 5-(4-((4-bromobenzyl)oxy)benzylidene)-1,3-dimethylpyrimidine-2,4,6(1H,3H,5H)-trione derivatives (**VI**) as DNA binding agents were evaluated [17]. According to the obtained results, the designed scaffold could bind to the DNA strand with Ka: 2.1×10^4 (M-1). To evaluate the role of N atoms in interaction with the DNA strand, we planned to synthesize 2–(4-(benzyloxy)benzylidene)cyclohexane-1,3-dione derivatives (**VII**) (Figure 2). In this regard, (benzyloxy) benzaldehydes (**3**) was reacted with 1,3-cyclohexanedione with an equal molar ratio. Unfortunately, our efforts to synthesize derivatives of **VII** were not successful, and instead of these compounds, xanthene-1,8-dione derivatives were synthesized. Stoichiometric changes in the reaction could not solve this problem. Surprised by outcomes obtained, we decided to use this opportunity to synthesize derivatives of xanthene-1,8-diones as DNA-binding agents.

The synthetic routes for the preparation of xanthene-1,8-dione derivatives containing the benzylic ether tail (**4a–q**) were illustrated in Scheme 1. For this purpose, the reaction between (benzyloxy)benzaldehydes (**3**) and 1,3-cyclohexanedione was carried out in ethylene glycol at 80°C to obtain the desired products **4a–q** in moderate to good yields. The structures of new xanthene-1,8-dione derivatives were confirmed by IR, ^{1}H NMR, and mass spectroscopy.

The mechanism of xanthine ring formation in the products is shown in Scheme 2. First, intermediate **VII** is formed by the condensation of one equivalent of 1,3-cyclohexanedione and aldehyde. Then the second equivalent of 1,3-cyclohexanedione reacts with intermediate **VII,** and after removing H_2O, the xanthene ring is formed.

Xanthene-1,8-dione products derived from 4-hydroxy benzaldehyde or vanillin are shown in Table 1.

3.2. ADME Prediction. All new derivatives (**4a–q**) of xanthene-1,8-dione were investigated to evaluate their drug-likeness via Lipinski's rule of 5. Data in Table 2 show that all compounds passed Lipinski's rule and met the criteria for drug-likeness.

To predict the drug-likeness properties of all xanthene-1,8-dione derivatives and also Daunomycin, the molecular weight (MW), the number of hydrogen bond acceptors (HBA) donors (HBD), the lipophilicity index (Clog P), and the rotatable bond count (RBC) were calculated according to Lipinski's rule of five. RO5 implies that molecules with MW ≤ 500, HBA ≤ 10, and HBD ≤ 5, ClogP ≤ 5, and RBC ≤ 10 have good absorption through oral administration [19].

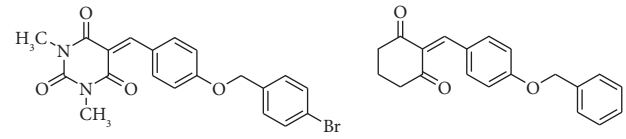

VI VII

Figure 2: Chemical structures of compounds VI and VII.

Daunomycin had a larger MW than the xanthene-1,8-dione derivatives that violated the RO5. But the high polarity of Daunomycin (ClogP = 0.92) could compensate for the violation of the MW criterion. The main differences between the drug-likeness profiles of Daunomycin and xanthene-1,8-dione derivatives were the number of HBDs and polarity. The xanthene-1,8-dione derivatives were lipophilic compounds (in comparison to Daunomycin) that did not have any HBD groups.

According to the obtained results, we concluded that the synthesized xanthene-1,8-dione derivatives were more lipophilic than approved anticancer drugs. This physicochemical property might help the entrances of molecules into the cells but decreases the selectivity profile of the proposed scaffold. Directional hydrogen bonds (donor or acceptor) orient drugs to form specific interactions in the binding site that lead to more selective drugs.

3.3. Biological Assay. Our results on the evaluation of the antitumor activity of the compounds **4a–q** against the lung cancer cell line (A549) are presented in Table 3. The results show that only compound **4a** has significant activity against A549 with an IC_{50} value 34.59 μMin comparison to Cisplatin as a reference antitumor agent [20] with an IC_{50} value 20.86 μM. It surprised us that the other derivatives did not have good activity against this cell line.

3.4. Docking Studies. Binding energies of Daunomycin and 4a with DNA strand D (CPGPTPAPCPG) calculated by the docking process are presented in Table 4. Self-docking of crystallographic ligand via the mentioned procedure led to an RMSD equal to 0.95 Å. The comparison of the predicted and crystallographic pose of Daunomycin showed minor deviation. Accordingly, we found that the molecular docking method was valid. Also, the validation was repeated for 3 times with different initial conformers of Daunomycin. Except for the population of the high-rank cluster (9.4% deviation), all the results were the same. Considering the obtained cytotoxic results, just compound **4a** was evaluated in a molecular docking study.

The comparison of the estimated free energy of binding after 106 bootstrapping cycles and the 95% confidence interval showed a significant difference in binding energy between Daunomycin and **4a**. The standard deviation of RMSD between conformers in the top cluster of Daunomycin and **4a** was $\pm 2.7 \times 10^{-2}$ and $\pm 5.8 \times 10^{-3}$, respectively. The larger conformational space of **4a** in the top cluster of the docking result was related to the structural variation of the benzyloxy tail in the minor groove of DNA. The

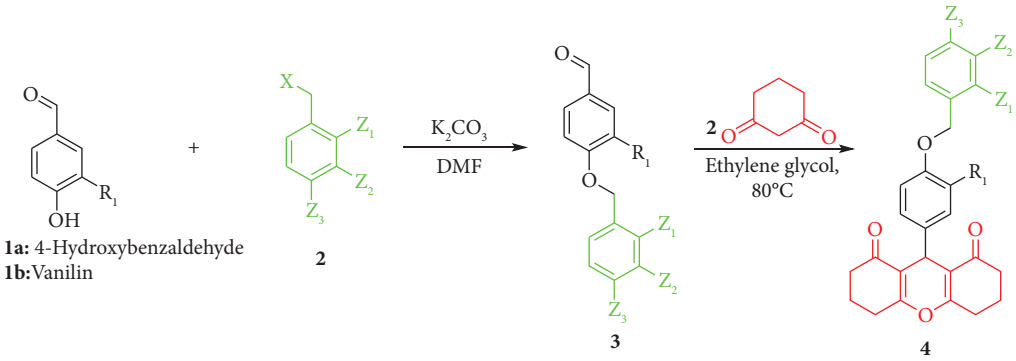

Scheme 1: Synthesis of xanthene-1,8-dione derivatives (4a–q).

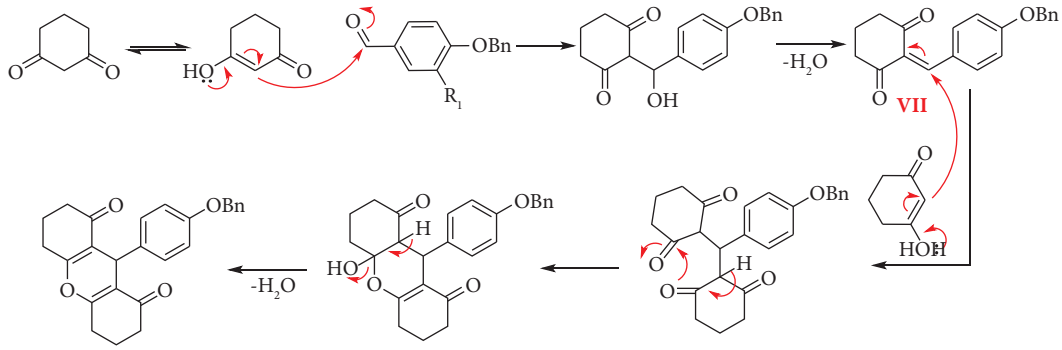

Scheme 2: Mechanism of xanthene ring formation.

Table 1: Xanthene-1,8-dione products derived from 4-hydroxy benzaldehyde (**4a**–**h**) or vanillin (**4i**–**q**).

Entry	Product	R_1	Z_1	Z_2	Z_3
1	**4a**	H	H	H	H
2	**4b**	H	H	H	Br
3	**4c**	H	H	Cl	H
4	**4d**	H	H	H	F
5	**4e**	H	F	H	H
6	**4f**	H	H	F	H
7	**4g**	H	H	H	CH_3
8	**4h**	H	H	H	Cl
9	**4i**	OCH_3	H	H	H
10	**4j**	OCH_3	H	H	Br
11	**4k**	OCH_3	H	Cl	H
12	**4l**	OCH_3	H	H	F
13	**4m**	OCH_3	F	H	H
14	**4n**	OCH_3	H	F	H
15	**4o**	OCH_3	H	H	CH_3
16	**4p**	OCH_3	H	H	Cl
17	**4q**	H	H	H	CN

difference in conformational variation affected the range of the confidence interval. Due to difference in the core structure of Daunomycin and **4a**, ligand efficiency was calculated to compare the participation of each atom in binding to DNA. Both ligands had the same LE (0.32 $kcalmol^{-1}$/heavy atoms). Although the designed xanthene-1,8-dione possessed fewer atoms and consequently more binding interactions than Daunomycin, the efficiency of the atoms of **4a** was higher than that of Daunomycin in the binding process.

The docking study of **4a** showed that the xanthene-1,8-dione ring intercalated between nucleobases (Figure 3). In this orientation, the phenoxybenzyl tail occupied the minor groove. Considering the predicted binding pose, the active

Table 2: Physicochemical properties of xanthene-1,8-diones.

Compound	Molecular weight (Da)	Rotatable bonds count (RBC)	Hydrogen bond acceptor (HBA)	Hydrogen bond donor (HBD)	Clog P
4a	400	4	4	0	3.75
4b	478	4	4	0	4.61
4c	434	4	4	0	4.46
4d	418	4	5	0	3.89
4e	418	4	5	0	3.89
4f	418	4	5	0	3.89
4g	414	4	4	0	4.25
4h	434	4	4	0	4.46
4i	430	5	5	0	3.49
4j	508	5	5	0	4.35
4k	464	5	5	0	4.20
4l	448	5	6	0	3.63
4m	448	5	6	0	3.63
4n	448	5	6	0	3.63
4o	444	5	5	0	3.99
4p	464	5	5	0	4.20
4q	425	4	5	0	3.18
Daunomycin	527.5	4	11	5	0.92

Table 3: The IC_{50} values of the xanthene-1,8-diones in MTT assay against A549 cell.

Complex	IC_{50} (μM)
4a	34.59 ± 1.84
4b	>100
4c	>100
4d	>100
4e	>100
4f	>100
4g	>100
4h	>100
4i	>100
4j	>100
4k	>100
4l	>100
4m	>100
4n	>100
4o	>100
4p	>100
4q	>100
Cis-platin	20.86 ± 4.25

Table 4: Binding energy of Daunomycin and 4a with DNA strand D (CPGPTPAPCPG). Energy is reported in Kcal mol^{-1}. The confidence interval was calculated by applying 106 cycles of bootstrapping.

Compound	Estimated free energy of binding ($kcalmol^{-1}$)	Mean binding energy ($kcalmol^{-1}$)	0.95% confidence interval ($kcalmol^{-1}$)	LE ($kcalmol^{-1}$/heavy atom)	RMSD (Å)
Daunomycin	−12.10	−12.06 (±0.034)	[−12.07, −12.05]	0.32	0.95
4a	−9.73	−9.54 (±0.14)	[−9.65, −9.43]	0.32	—

conformation of xanthene-1,8-dione derivatives depends on the hybridization of the C4 atom (SP^3) in pyran ring. The amino group of aminoglycoside in Daunomycin is essential for binding to DNA. The amino moiety in addition to the hydrogen bond with DC can form ionic interaction with negatively charged phosphate groups. The same interaction could be achieved in xanthene-1,8-dione derivatives by substituting appropriate basic groups at the *ortho* position of benzyl or the *meta* position of phenoxy.

We found that the cytotoxic effect of xanthene-1,8-dione derivatives has a high dependency on substitution at different positions. According to docking results, we proposed

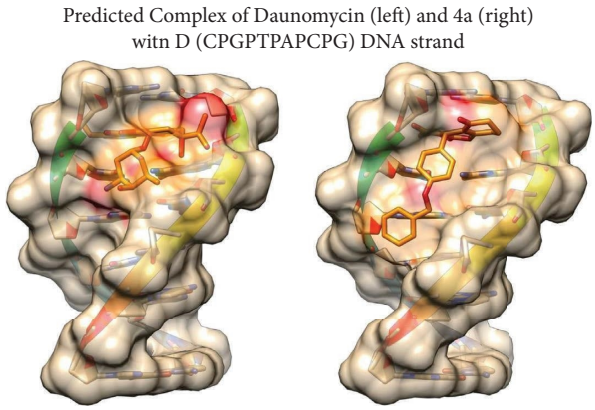

Figure 3: Orientation of Daunomycin and **4a** in complex with D(CPGPTPAPCPG) DNA strand. Ligands are shown by orange sticks. The proper substitutions at meta position of phenoxy or ortho position of benzyl can occupy the same binding region of aminoglycoside.

that adding a basic functional group at the metaposition of phenoxy or orthoposition of benzyl moieties could improve binding affinity and the physicochemical properties of the designed xanthene-1,8-dione derivatives.

4. Conclusion

Seventeen new xanthene-1,8-dione derivatives were synthesized and evaluated in the MTT assay against A549 cancer cell line. Compound 9-(4-(benzyloxy)phenyl)-3,4,5,6,7,9-hexahydro-1H-xanthene-1,8(2H)-dione (**4a**) showed good cytotoxic effects on this cell line (IC50: $34.59 \pm 1.84\,\mu$M). Also molecular docking results indicated that 4a could interact with the DNA strand the same as Daunomycin via an intercalating mechanism. Based on the results, it can be concluded that compound **4a** is a potential DNA-binding agent. However, the confirmation of the conclusion depends on experimental studies.

Data Availability

Data used in this study are available in supplementary information files.

Conflicts of Interest

The authors declare that there are no conflicts of interest.

Acknowledgments

This project was supported by the Research and Technology Vice-Chancellor of Hamadan University of Medical Sciences with grant no. 9908205898 related to Karimi's thesis.

Supplementary Materials

Supplementary information including IR, 1H NMR, and MS spectra is available at the Journal of Chemistry site. The supplementary file containing the original analysis spectra (FTIR, ^{1}H NMR, ^{13}C-NMR, and mass spectra) is available in the Supplementary Materials file. (*Supplementary Materials*)

References

[1] J. Saffari Chaleshtori, S. H. Mortazavi, E. Heidari Sureshjani, and K. G. Samani, "In silico study of the effect of thymoquinone on three pre-apoptotic factors of bad, bak, and bim," *Avicenna Journal of Pharmaceutical Research*, vol. 1, no. 1, pp. 5–9, 2020.

[2] R. Palchaudhuri and P. J. Hergenrother, "DNA as a target for anticancer compounds: methods to determine the mode of binding and the mechanism of action," *Current Opinion in Biotechnology*, vol. 18, no. 6, pp. 497–503, 2007.

[3] S. H. Alotaibi and A. A. Momen, "Anticancer drugs' deoxyribonucleic acid (DNA) interactions," *Biophysical Chemistry-Advance Applications*, IntechOpen, London, UK, 2019.

[4] H. Arai, T. Yamauchi, K. Uzui, and T. Ueda, "Leukemia cells are sensitized to temozolomide, carmustine and melphalan by the inhibition of O^6-methylguanine-DNA methyltransferase," *Oncology Letters*, vol. 10, no. 2, pp. 845–849, 2015.

[5] S. U. Rehman, T. Sarwar, M. A. Husain, H. M. Ishqi, and M. Tabish, "Studying non-covalent drug–DNA interactions," *Archives of Biochemistry and Biophysics*, vol. 576, pp. 49–60, 2015.

[6] E. N. Ogbonna, A. Paul, J. Ross Terrell et al., "Drug design and DNA structural research inspired by the Neidle laboratory: DNA minor groove binding and transcription factor inhibition by thiophene diamidines," *Bioorganic and Medicinal Chemistry*, vol. 68, Article ID 116861, 2022.

[7] S. Venugopal, V. Sharma, A. Mehra, I. Singh, and G. Singh, "DNA intercalators as anticancer agents," *Chemical Biology and Drug Design*, vol. 100, no. 4, pp. 580–598, 2022.

[8] Q.-Y. Nie, Y. Hu, X.-F. Hou, and G.-L. Tang, "Biosynthesis of DNA-alkylating antitumor natural products," *Molecules*, vol. 27, no. 19, p. 6387, 2022.

[9] J. Fotie and D. S. Bohle, "Pharmacological and biological activities of xanthones," *Anti-Infective Agents in Medicinal Chemistry*, vol. 5, no. 1, pp. 15–31, 2006.

[10] R. Giri, J. R. Goodell, C. Xing et al., "Synthesis and cancer cell cytotoxicity of substituted xanthenes," *Bioorganic and Medicinal Chemistry*, vol. 18, no. 4, pp. 1456–1463, 2010.

[11] D. Kumar, P. Sharma, H. Singh et al., "The value of pyrans as anticancer scaffolds in medicinal chemistry," *Royal Society of Chemistry Advances*, vol. 7, no. 59, pp. 36977–36999, 2017.

[12] R. Sangwan, M. Saini, R. Verma, S. Kumar, M. Banerjee, and S. Jain, "Synthesis of 1, 8-dioxooctahydroxanthene derivatives using ionic liquids, quantum chemical studies and anticancer activity," *Journal of Molecular Structure*, vol. 1208, Article ID 127786, 2020.

[13] Z. Najafi, A. Kamari-aliabadi, R. Sabourian, M. Hajimahmoodi, and G. Chehardoli, "Synthesis and molecular modeling of new 2-benzylidenethiobarbituric acid derivatives as potent tyrosinase inhibitors agents," *Journal of the Chinese Chemical Society*, vol. 69, no. 4, pp. 692–702, 2022.

[14] A. Bahmani, Z. Najafi, and G. Chehardoli, "Curcumin-derived heterocycles as anticancer agents. A systematic review," *Organic Preparations and Procedures International*, vol. 54, no. 6, pp. 493–510, 2022.

[15] S. Babaee, G. Chehardoli, T. Akbarzadeh et al., "Design, synthesis, and molecular docking of some novel tacrine based cyclopentapyranopyridine- and tetrahydropyranoquinoline-kojic acid derivatives as anti-acetylcholinesterase agents," *Chemistry and Biodiversity*, vol. 18, no. 6, Article ID e2000924, 2021.

[16] G. Chehardoli and A. Bahmani, "Synthetic strategies, SAR studies, and computer modeling of indole 2 and 3-carboxamides as the strong enzyme inhibitors: a review," *Molecular Diversity*, vol. 25, no. 1, pp. 535–550, 2021.

[17] A. Ebadi, Z. Najafi, H. Pakdel-yeganeh, D. Dastan, and G. Chehardoli, "Design, synthesis, molecular modeling and DNA-binding studies of new barbituric acid derivatives," *Journal of the Iranian Chemical Society*, vol. 19, no. 9, pp. 3887–3898, 2022.

[18] A. H. J. Wang, G. Ughetto, G. J. Quigley, and A. Rich, "Interactions between an anthracycline antibiotic and DNA: molecular structure of daunomycin complexed to d(CpGpTpApCpG) at 1.2-.ANG. resolution," *Biochemistry*, vol. 26, no. 4, pp. 1152–1163, 1987.

[19] C. A. Lipinski, F. Lombardo, B. W. Dominy, and P. J. Feeney, "Experimental and computational approaches to estimate solubility and permeability in drug discovery and development settings," *Advanced Drug Delivery Reviews*, vol. 64, pp. 4–17, 2012.

[20] E. H. Al-Rikabi, R. A. Al-Refai, S. J. Baqir, A. G. Hadi, and A. K. Al-Q, "Synthesis, structure, and in vitro cytotoxic activity of two organotin complexes of 2-[(2, 3-dimethylphenyl) amino] benzoic acid," *Journal of Medicinal and Chemical Sciences*, vol. 6, pp. 1230–1238, 2023.